

Requirement of Mixed Lineage Kinase 3 CRIB domain for
maintenance of basal cardiac homeostasis and left
ventricular function after pressure overload

A thesis submitted by

Peiwen Liu

In partial fulfillment of the requirements for the degree of

Master of Science

In

Pharmacology and Drug development

Tufts University

Graduate School of Biomedical Sciences

May 2020

Advisor: Robert Blanton, MD

Abstract

Cardiovascular disease remains a leading cause of mortality worldwide. From previous research, we know that the cGMP-PKG pathway is important in opposing development of cardiac hypertrophy and subsequent heart failure, but the downstream PKG effectors mediating this remain unknown. Prior studies reveal that the c-Jun NH₂-terminal kinase (JNK) signaling pathway opposes cardiac remodeling. In the previous study, we found that mice with whole body deletion of the JNK-activating protein MLK3 have more significant cardiac dysfunction and remodeling, especially after pressure overload. Activation of MLK3 kinase requires the interaction of the small GTPase cdc42 with the MLK3 cdc42/Rac-interactive binding (CRIB) motif. To determine the MLK3 kinase dependent and independent mechanism of regulating the cardiovascular pathological processes, we designed the present study using a novel animal model. In this study, mice with whole body mutation of the MLK3 CRIB domain, leading to impaired cdc42-mediated MLK3 activation were measured in the baseline state, and in response to LV pressure overload by transaortic constriction (TAC). We observed increased cardiac hypertrophy and hypertension in mutant mice. When checking the protein expression, the MLK3 protein level, the activation of JNK protein and the CD31 protein expression were lower in MLK3 CRIB mice, compared with wild type littermate controls. After 25G TAC for 1 week, the MLK3 CRIB mutant mice developed worsened cardiac dysfunction, increased LV wall thickness, but no differences in organ weights. These data demonstrated a critical role of the MLK3 CRIB domain in the regulation of blood pressure, LV hypertrophy, and LV compensation to pressure overload in vivo.

Table of Contents

Title Page	i
Abstract	ii
Table of Contents	iii
List of Tables	iv
List of Figures	v
List of Abbreviations	vi
Chapter 1: Introduction	1
Chapter 2: Methods	6
2.1 Study approval and experimental animals	6
2.2 Echocardiography	6
2.3 Transverse aortic constriction (TAC)	7
2.4 Pressure Volume-hemodynamic measurements (PV-loops)	7
2.5 Tissue isolation	8
2.6 Western blotting	8
2.7 Statistics analysis	10
Chapter 3: Results	11
3.1 MLK3 CRIB mice exhibit basal cardiac hypertrophy	11
3.2 Normal baseline cardiac structure and function in MLK3 CRIB mutant mice	13
3.3 Baseline cardiac function measurement	15
3.4 Decreased activation of JNK pathway in the LV from MLK3 CRIB mice	16
3.5 Organ weight preserved in MLK3 CRIB mice after pressure overload	17
3.6 Higher blood pressure in the female MLK3 CRIB mice after TAC	19
3.7 Decreased cardiac function in MLK3 CRIB mutant mice	20
3.8 Statement of Contributions	21
Chapter 4: Discussion	24
Chapter 5: Bibliography	28

List of Tables

Table 3.1 Baseline organ masses in MLK3 CRIB and MLK3 wild type mice	12
Table 3.2 Baseline cardiac structure and function in MLK3 CRIB and MLK3 wild type mice.....	14
Table 3.3 Baseline hemodynamic analysis in MLK3 CRIB and MLK3 wild type mice .	15
Table 3.4 Organ weights analysis in MLK3 CRIB and wild type mice after 25G TAC ..	18
Table 3.5 Hemodynamic analysis in MLK3 CRIB and wild type mice after 25G TAC ..	22
Table 3.6 Cardiac structure and function in MLK3 CRIB and wild type mice after 25G TAC.....	23

List of Figures

Figure 3.1 Baseline ventricle weight analysis in different gender in MLK3 CRIB (C/C) and wild type (+/+) mice.....	11
Figure 3.2 Baseline cardiac structure and function measured by Echo in MLK3 CRIB (C/C) and wild type (+/+) mice.....	13
Figure 3.3 Baseline hemodynamic analysis in MLK3 CRIB (C/C) and wild type (+/+) mice displayed by gender.....	14
Figure 3.4 Western blot and quantification of JNK, CD31 and MLK3 in heart in MLK3 CRIB (C/C) and wild type (+/+) mice	16
Figure 3.5 Hemodynamic analysis and ventricle weight analysis in MLK3 CRIB (C/C) and wild type (+/+) mice after TAC	19
Figure 3.6 Cardiac function analysis in MLK3 CRIB (C/C) and wild type (+/+) mice by echocardiography after TAC.....	20

List of Abbreviations

cGMP	The second messenger cyclic guanosine monophosphate
CRIB	MLK3's cdc42/Rac-interactive binding motif
DBP	Diastolic blood pressure
Echo	Echocardiography
EF	Ejection Fraction
FS	Fractional Shortening
GC	Guanylate cyclase
HF	Heart Failure
HR	Heart Rate
IVS;d	End-diastolic septum thickness, end-diastolic
JNK	c-Jun NH ₂ -terminal kinase
LV	Left ventricle
LVIS;d	Left ventricular internal dimension, end-diastolic
LVPW;d	Left ventricular posterior wall thickness, end-diastolic
MLK3	Mixed lineage kinase-3
NPs	Natriuretic peptides
PKG	The cGMP dependent protein kinase
RV	Right ventricle
SBP	Systolic blood pressure
SH3	Src homology 3
TAC	Transvers aortic constriction
PV-loops	Pressure Volume-Loops

Chapter 1: Introduction

Cardiovascular disease remains the number one cause of adult mortality worldwide, irrespective of age, gender, and ethnicity (1). Within the broader scope of cardiovascular disease, heart failure is the most common cause of cardiovascular death. Pressure overload represents a common cause of heart failure (HF). Specifically, in response to pathological stimuli to the left ventricle, cardiomyocytes become hypertrophic which initially preserves normal cardiac output. Ultimately, however, this hypertrophic process also increases the risk of heart failure (HF) (2, 3). Current treatments for HF include medications, dietary interventions, devices, and surgical treatment such as transplants, but the prognosis for HF remains poor (4). In the field of HF, one research goal is to identify specific genes and gene products regulating both the development of hypertrophy and of LV dysfunction and remodeling, in order to identify potential novel therapeutic targets for HF.

The cyclic GMP- dependent protein kinase (PKG) intracellular signaling pathway is a ubiquitous second messenger system which has been established as opposing development of a number of heart diseases, including LV hypertrophy and HF. PKGI inhibits pathological cardiac hypertrophy and remodeling in response to pressure overload (5,6). Although there are two PKG genes, only PKGI is found to be expressed in cardiac system. To activate PKG in ventricular cardiomyocytes, an upstream PKGI activation pathway has been identified. First, cGMP is generated by one of two guanylate cyclases (GC), the soluble GC (sGC) or particulate GC (pGC). The sGC is stimulated by NO diffusing directly across

the plasma membrane; while pGC, a membrane bound receptor, is activated by extracellular NPs. Then the cyclic GMP (cGMP), which is synthesized by GC, directly activates PKGI, which causes the vasodilation in cardiovascular system (5, 7). The PKGI gene expresses as two isoforms: PKGI α and PKGI β . They both have unique N-terminal leucine zipper (LZ) interaction domains which differ in sequence from one another. These LZ domains mediate PKGI binding to critical substrates, many of which also contain similar LZ domains (7). The Blanton lab has investigated PKGI α LZ-dependent binding molecules as a strategy to elucidate the downstream substrates of PKG and thus potential novel anti-remodeling molecules.

The c-Jun N-terminal Kinase (JNK) pathway has been shown to be involved in cardiometabolic factors which include inflammation, insulin resistance, immune cell differentiation, and other processes (8). There are three isoforms of JNK encoded by three separate genes, JNK1 (Mitogen Protein Kinase 8(MAPK8), JNK2 (MAPK9), and JNK3 (MAPK10), while only JNK1 and JNK2 are found to be expressed in myocardium JNK3 is expressed in brain and nerves. JNK is activated both when injury as well as cardioprotective response occurs in the heart (9). In multiple cell types, external stresses such as UV radiation, reactive oxygen species (ROS), and free fatty acids (FFA) activate upstream MAP kinases leading to JNK cascade activation. JNK can be activated by multiple different upstream pathways. MAP3Ks, including MLKs (mixed lineage kinase), activate the JNK in response to free fatty acids (FFA), ceramide, and the cytokine TNF α , which causes further activation of MAP2Ks family (MKK4 and MKK7) through

phosphorylation (8, 10, 11). MKKs at the plasma membrane initiate the JNK branch and promote activation of dual-specificity kinases MKK4 and MKK7, which then activates JNK through phosphorylation of Thr and Tyr residues in a Thr-Pro-Tyr (TPY) motif of JNK kinases (12,13).

In previous work, we demonstrated that genetic disruption of the PKG pathway blocks JNK activation in the LV after TAC, but the specific PKGI substrates required for PKG activation of JNK still remain unclear. We therefore screened the upstream signaling molecules of JNK activation, and we hypothesized that MLK3 is one of the substrates of PKG required for this mechanism.

MLK3, a mitogen-activated protein kinase, also called Src homology 3 (SH3) domain-containing proline-rich kinase, is a master upstream regulator of the JNK pathway (14). MLK3 also phosphorylates other substrates including I κ B kinase α (IKK α) and IKK β , which activate the NF- κ B pathway (15). Studies have identified several important domains in MLK3, including a Src homology 3 (SH3) domain, a leucine zipper, and a Cdc42/Rac interactive binding (CRIB) motif.

When activated, Cdc42 binds to the MLK3 CRIB motif which then induces MLK3 autophosphorylation, leading to increased MLK3 catalytic activity (16, 17, 18). When inactive, MLK3 is autoinhibited through its SH3 domain. To activate the MLK3 kinase, it requires the interaction of Cdc42 with MLK3's CRIB motif and resulting in the displacement of MLK3's SH3 domain. Kinase activation occurs through two steps: autophosphorylation of Thr277 and Ser281 and dimerization via the MLK3 leucine zipper domain (19). Once activated, MLK3 binds and phosphorylates downstream substrates, including the mitogen-activated

kinase kinases MKK4/7 and MKK3/6, which then in turn phosphorylate the MAP kinases JNK, ERK or p38. This is the kinase- dependent mechanism of MLK3 signaling.

Despite the molecular understanding of MLK3 kinase activation and effectors, the specific role of MLK3 in cardiac signaling still remains unclear. Our lab therefore first investigated a MLK3 whole body knock out model and measured the cardiac function and structural phenotypes both in the baseline state, and after pressure overload model (3). The whole body MLK3 knockout mice showed baseline cardiac hypertrophy with preserved cardiac function. After left ventricle pressure overload, knockout mice developed more severe left ventricle hypertrophy compared to the wild type mice. These findings indicate that MLK3 normally opposes cardiac remodeling and hypertrophy, and therefore that MLK3 may be a potential therapeutic target for the treatment or prevention of HF. We designed the current study to test the requirement of the MLK3 CRIB motif in the inhibition of basal and pressure overload-induced LV hypertrophy and dysfunction. To do this, we investigated a mouse model with mutation in the MLK3 CRIB domain, which may impair the interaction of MLK3 CRIB motif with SH3 domain and cause the inactivation of MLK3 (20). We hypothesized that MLK3 CRIB mutant mice might show a similar pathological impairment and dysfunction in hearts compared to MLK3 knockout mice, which would support the hypothesis that MLK3 CRIB domain is important for MLK3 kinase function in the cardiovascular system. In this study, we investigated cardiac structure and

function of the CRIB mutant mice both in the baseline state and in response to left ventricle pressure overload.

Chapter 2: Methods

2.1 Study approval and experimental animals

All rodent care and procedures were approved by the Institutional Animal care and Use Committee of Tufts Medical Center. Whole body MLK3 gene CRIB domain mutant mice were provided by our collaborators Dr. Roger Davis (PhD, School of Medicine, University of Massachusetts, Worcester, MA) and were bred in the animal facility at Tufts medical center (Boston, MA). These mice harbor two points mutations within the MLK3 CRIB domain which abolishes cdc42 binding to MLK3 and disrupts cdc42-mediated MLK3 kinase activation and plasma membrane translocation. 12 to 15 week-old animals were assigned to two different groups depending on their genotypes (wild type or MLK3 CRIB). Both the wild type and MLK3 CRIB mice came from the same strain, and we used littermates in all studies. All experimental mice were maintained on a C57BL/6 background (12:12 hour light-dark cycle at 22±2 °C in the animal facility at Tufts medical center (Boston, USA)). Only male and female 10- to 15- week-old mice were used for these studies. Investigators were blinded to animal genotype before the animal surgeries.

2.2 Echocardiography

Cardiac function of experimental animals was obtained by echocardiography. For the baseline study, echocardiograms were performed within 3 days before the Pressure Volume analysis and harvest. For the subsequent transaortic constriction (TAC) study, echocardiograms were done within 3 days before surgery, and also on the day before the PV-loops and harvest. Mice were anesthetized with 2.5%

gaseous isoflurane in medical oxygen at 1L/minute, then maintained under 1-2% isoflurane in the supine position. Chest fur was removed with hair remover (Nair, USA), Excessive cream was removed by damp cotton pad. Ultrasonic gel was applied to the echocardiography transducer (MS550D; Vevo 2100, FUJIFILM VisualSonics, Canada), and scanning performed through the long and short- axis view in M-mode and B-mode. All the echocardiographs were obtained and analyzed by one echocardiographer and the same machine. For the TAC group, the color Doppler imaging was also be done to check the blood flow velocity in aortas after TAC on the day before doing PV-loops. All the measurements were done for three times per mouse and averages were calculated for each parameter.

2.3 Transverse aortic constriction (TAC)

Only 10- to 15- week-old mice were used in 25 Gauge TAC study. Both wild-type and MLK3 CRIB mice underwent TAC surgery as preciously described (21). Briefly, mice were anesthetized with 2.5% gaseous isoflurane, intubated and maintained on a small animal ventilator, before thoracotomy. Following surgery were performed using a 25-gauge needle (0.51 mm outer diameter) which was tied around the transverse aorta between the two carotid arteries.

2.4 Pressure Volume-hemodynamic measurements (PV-loops)

Left ventricular function was also analyzed through simultaneous measurement of LV pressure and volume in vivo to generate pressure-volume loops. For the baseline group, PV-loops were done when the mice were 12 to15-week-old. While for the TAC study, PV-loops were done 7-days after the 25G TAC surgery. Mice were anesthetized with 3.0% gaseous isoflurane and maintained at 2.0%

isoflurane. The body temperature was maintained and monitored via a rectal thermometer- lamp system. A 1.0 F catheter was placed in the left ventricle through the carotid and the aortic arch. The data was obtained and analyzed with IOX version 2.1.10 software (EMKA instruments).

2.5 Tissue isolation

Following pressure-volume hemodynamic measurements, selected organs (hearts, lungs, livers, kidney) were harvested and the tibia length was measured in order to normalize organ mass to body size. After weighing, the heart was excised into 4 chambers and atria were removed and stored separately. The left ventricle was divided along the short axis into 3 pieces: apex, base and middle. The middle LV section was stored in 5% formalin for histological measurements. Other parts of heart as well as other organs were snap frozen in liquid nitrogen and stored at -80-degrees.

2.6 Western blotting

Tissues were frozen in liquid nitrogen immediately after harvest and stored under -80-degree condition. Tissues were crushed on dry ice without thawing until the tissue became powder. Tissue powder was lysed with tissue lysis buffer (20 mmol/l HEPES, 50 mmol/l beta-glycerol phosphate, 2 mmol/l EGTA, 1 mmol/l DTT, 10 mmol/l NaF, 1 mmol/l NaVO₄, 1% Triton X-100, and 10% glycerol), supplemented with 1mmol/l PMSF. Next, 200 µl of lysis buffer was added per 10 mg tissue powder followed by vortexing the mixture for at least 20 seconds per sample. Samples were kept on ice for 1 hour, while tapping and rotating the samples every 20 minutes. Lysates were cleared by the highest speed

centrifugation and the supernatant was saved. Protein concentrations were quantified by BCA assay (Thermo Scientific, JD120868) and lysates were diluted in 2X Laemmli sample buffer (Sigma S-3401). Protein samples (30 ug/well) and protein ladder marker (Bio-Rad Precision Plus Dual Color Standards no. 161-0374) were loaded into 8% or 12% polyacrylamide gels and transferred to Nitrocellulose membranes (Bio-Rad, no. 1620094). After staining with Ponceau S to check the efficiency after transfer, membranes were washed with TBST and incubated in 5% blocking buffer (Blotting-Grade Blocker, Bio-Rad, 1706404) for 1 hour. The membranes were incubated in different primary antibodies for 1 hour at room temperature or over-night in 4°C cold room. We used the following antibodies for this study: MLK3 (Abcam, ab51068), GAPDH (EMD Millipore, MAB374), phosphorylated JNK (Cell Signaling Technology, no. 4668), JNK (Cell Signaling Technology, no. 9252). After incubation with primary antibody, membranes were incubated in secondary anti-rabbit antibodies (GE Healthcare, NA934) for 1 hour in room temperature. After incubating in the ECL substrate (ThermoFisher Scientific, no. 34095) membranes were visualized by ProteinSimple FluorChem E system, and the quantification of the detectable bands was done by using the Alpha Innotech Imager software. The analysis of the bands of specific proteins were normalized by the quantification of the GAPDH on the same membrane.

2.7 Statistics analysis

All data is presented as mean \pm standard error of the mean, and the statistics are performed with a two-tailed unpaired t-test. Values of $P < 0.05$ were considered statistically significant.

Chapter 3: Results

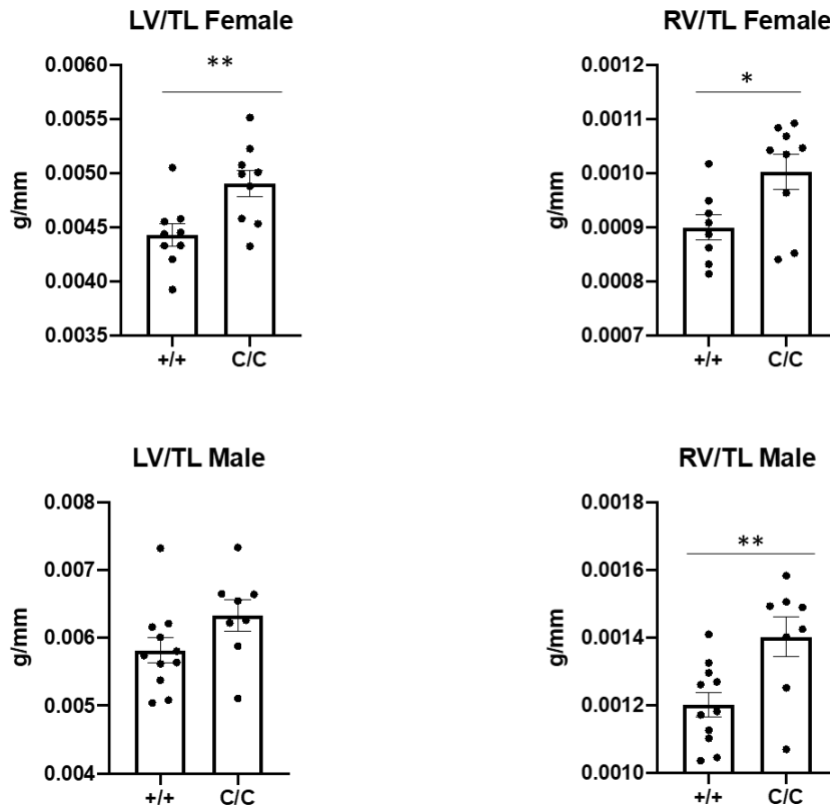


Figure 3.1 Baseline ventricle weight analysis in different gender in MLK3 CRIB (C/C) and wild type (+/+) mice

3.1 MLK3 CRIB mice exhibit basal cardiac hypertrophy

We first analyzed the body weights and the organ weights of the MLK3 CRIB mice and wild type littermates. Baseline organ masses of male and female MLK3 CRIB mice demonstrated increased LV mass compared with control mice. When normalized with tibia length (TL), there was still increase in LV, RV and atria weight in MLK3 CRIB mice compare to wild type mice, which indicates there was hypertrophy not only in left ventricle, but also the whole heart. This weight difference between MLK3 CRIB mice and wild type mice might indicate that mice with impaired MLK3 kinase activation may have developed cardiac

dysfunction during growth, and also support the hypothesis that MLK3 plays a role in the prevention of cardiac dysfunction and remodeling (Table 3.1, Figure 3.1).

Table 3.1 Baseline organ masses in MLK3 CRIB and MLK3 wild type mice

	MLK3 CRIB	MLK3 WT	P Value
Male			
n	8	11	
BW, g	27.0±0.8	28.7±0.6	0.12
LV, mg	107.8±3.8	100.9±3.7	0.23
RV, mg	23.8±1.0	20.8±0.6	0.02
Atria, mg	7.4±0.4	8.9±0.5	0.30
LV/TL, mg/cm	63.3±2.3	58.2±1.9	0.10
RV/TL, mg/cm	14.0±0.6	12.0±0.3	0.007
Atria/TL, mg/cm	4.3±0.2	5.1±0.2	0.04
Female			
n	9	9	
BW, g	22.0±0.7	21.8±0.4	0.85
LV, mg	83.2±2.3	76.1±2.0	0.03
RV, mg	17.4±0.6	15.9±0.6	0.21
Atria, mg	6.0±0.4	6.5±0.3	0.01
LV/TL, mg/cm	49.0±1.2	44.3±1.0	0.009
RV/TL, mg/cm	10.0±0.3	9.2±0.3	0.12
Atria/TL, mg/cm	3.5±0.2	3.8±0.1	0.34
All Gender			
n	17	20	
LV/TL, mg/cm	55.7±2.1	51.9±1.9	0.20
RV/TL, mg/cm	11.9±0.6	10.7±0.3	0.11
Atria/TL, mg/cm	3.9±0.1	4.5±0.2	0.40

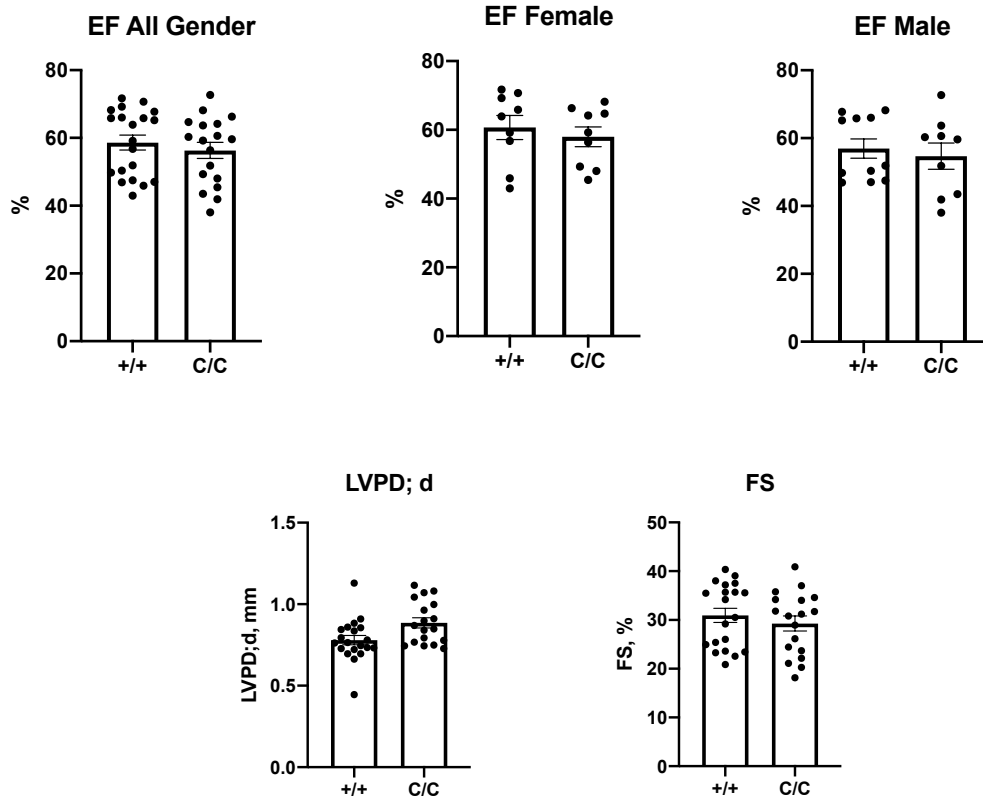


Figure 3.2 Baseline cardiac structure and function measured by Echo in MLK3 CRIB (C/C) and wild type (+/+) mice

3.2 Normal baseline cardiac structure and function in MLK3 CRIB mutant mice

Baseline cardiac structure and function was evaluated by echocardiography.

MLK3 CRIB mice displayed similar LV ejection fraction and fractional shortening when compared to wild type, which indicates the mutants have preserved cardiac function. For the LV chamber internal dimensions measured by M-mode, echocardiography, the wall-thickness (end-diastolic septum thickness, IVS;d; left ventricular internal dimension at end-diastolic, LVIS;d; left ventricular posterior wall thickness at end- diastolic, LVPW;d) measured during diastole were slightly increased in MLK3 CRIB mice (Table 3.2). This may indicate the left ventricle wall was slightly hypertrophic in MLK3 CRIB mice. In sum, the

MLK3 CRIB mice have preserved cardiac function and structure, but they also had slight pathological structure change in left ventricle, which further supporting the presence of adverse LV remodeling.

Table 3.2 Baseline cardiac structure and function in MLK3 CRIB and MLK3 wild type mice

	MLK3 CRIB	MLK3 WT	P Value
n	18	20	
Ejection Fraction, %	56.3±2.37	58.6±2.20	0.479
Fractional Shortening, %	29.27±1.53	30.93±1.50	0.441
IVS; d, mm	0.97±0.03	0.89±0.03	0.075
LVID; d, mm	3.79±0.05	3.38±0.07	0.097
LVID; s, mm	2.69±0.09	2.73±0.09	0.751
LVPW; d, mm	0.89±0.03	0.78±0.03	0.016
Heart Rate, beats/min	417±10.9	393±11.7	0.145

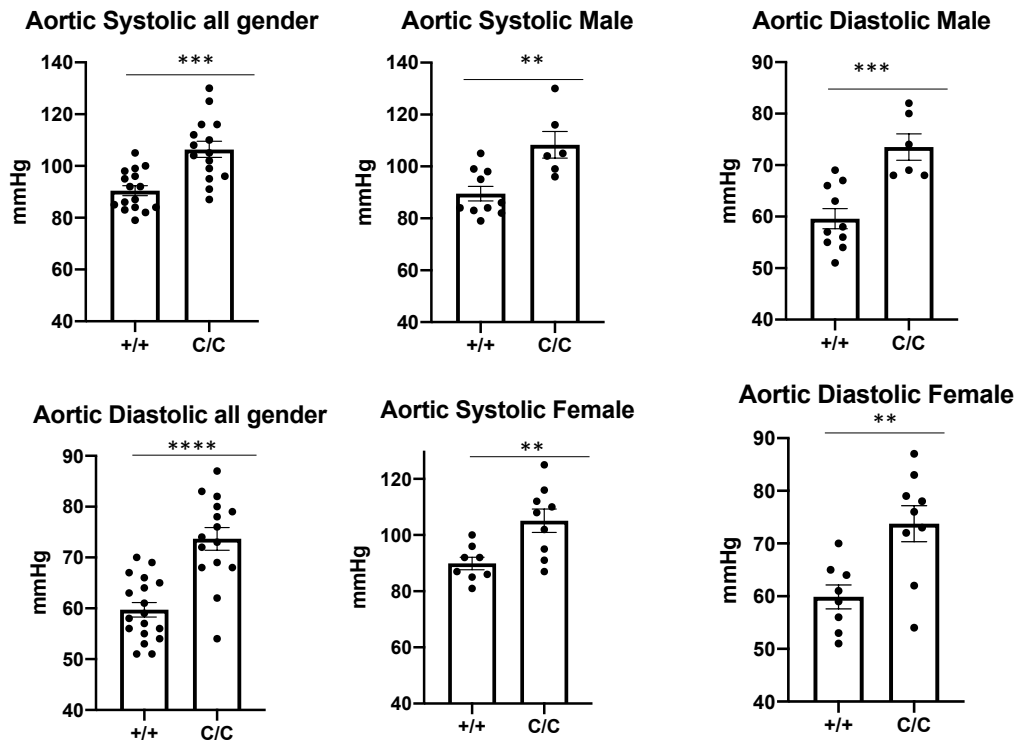


Figure 3.3 Baseline hemodynamic analysis in MLK3 CRIB (C/C) and wild type (+/+) mice displayed by gender

Table 3.3 Baseline hemodynamic analysis in MLK3 CRIB and MLK3 wild type mice

	MLK3 CRIB	MLK3 WT	P Value
n	15	18	
SBP, mmHg	106±3.1	89.7±1.8	<.001
DBP, mmHg	73.6±2.2	59.7±1.4	<.001
MA, mmHg	99.9±4.7	82.3±2.7	0.02
LV EDP, mmHg	5.2±1.3	6.2±1.3	0.57
LV Dp/dt _{max} , mmHg/s	7472±764	5415±413	0.20
LV Dp/dt _{min} , mmHg/s	-6264±696	-4751±696	0.06
Contractile index, s ⁻¹	182±9.1	191±7.8	0.44
Stroke Volume, µl	18.31±2.3	19.8±2.2	0.64
Cardiac Output, µl/min	8253±1106	8409±937	0.91

3.3 Baseline cardiac function measurement

Baseline cardiac function was also evaluated by invasive measurement of LV pressure and volume. There was significant elevation in systolic blood pressure (SBP) and diastolic blood pressure (DBP), measured in the aorta, in MLK3 CRIB mice, compared to wild type mice, regardless of gender. The other parameters were measured in left ventricle, and they indicated no basal difference in hemodynamics in left ventricle between genotypes. As the previous study showed (3), the whole body MLK3 knockout mice also showed higher baseline blood pressure. This may illustrate that MLK3 helps in regulating blood pressure, and more importantly, that the CRIB domain is required for this function in vivo (Table 3.3, Figure 3.3).

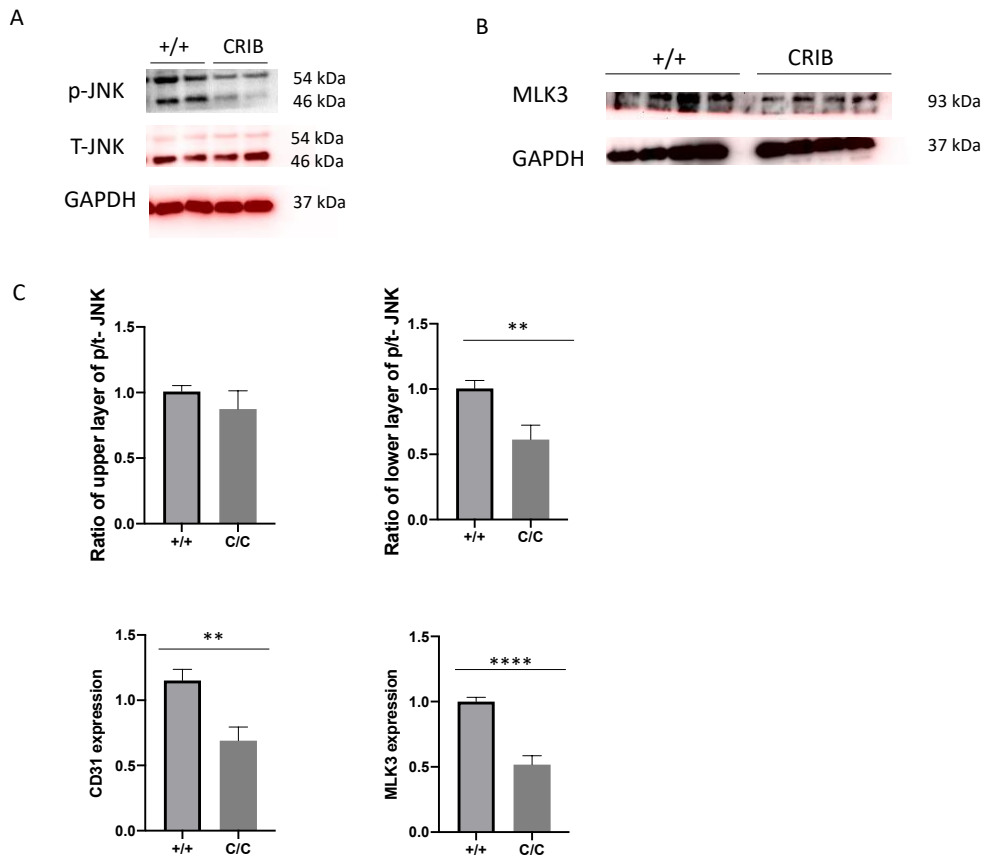


Figure 3.4 Western blot and quantification of JNK, CD31 and MLK3 in heart in MLK3 CRIB (C/C) and wild type (+/+) mice

3.4 Decreased activation of JNK pathway in the LV from MLK3 CRIB mice

After the physical cardiac structural and functional analysis, we next examined expression and activation state of selected proteins in the LV of MLK3 CRIB and wild type controls. Total MLK3 expression was lower in MLK3 CRIB group compared to wild type, indicating the CRIB domain has influence on MLK3 gene expression. We next assayed the JNK activation state in MLK3 CRIB and wild type mice. Though the total JNK (t-JNK) protein expression in the two genotypes did not differ significantly between genotypes, phosphorylated-JNK (p-JNK) was reduced in CRIB mutants, compared with WT controls, consistent with reduced

JNK activation in MLK3 CRIB mice. Also, the MLK3 CRIB group expressed less CD31 as compared to the wild type group, which is consistent with reduced LV capillary density. Together, these findings indicate that the CRIB domain plays an important role for MLK3 kinase regulation of molecular signaling and capillary density (Figure 3.4).

3.5 Organ weight preserved in MLK3 CRIB mice after pressure overload

We next examined the response of the MLK3 CRIB mutant mice to LV pressure overload. After 7 days of 25G TAC surgery, the basic cardiac structure and function was measured through PV-loops and weight of the organs. As Table 3.4 shows, the body weights were lower in MLK3 CRIB TAC mice compared with wild type, while the LV weight normalized to tibia length did not differ significantly in CRIB group compared with WT, especially in the male mice. When compared to the baseline, the ventricles weighed more after TAC surgery, which indicated the TAC surgery did cause pressure overload and also causes hypertrophy in left ventricle in wildtypes as well as mutants (Table 3. 4, Figure 3.5). Together, these data illustrated the MLK3 CRIB mice had reduced body weight but still develop LV hypertrophy.

Table 3.4 Organ weights analysis in MLK3 CRIB and wild type mice after 25G

TAC

	MLK3 CRIB	MLK3 WT	P Value
	Male		
n	9	7	
BW, g	26.5±0.8	29.0±0.5	0.04
LV, mg	124.0±4.8	132.7±3.7	0.19
RV, mg	24.1±0.9	24.6±1.4	0.78
Atria, mg	8.3±0.5	10.0±0.7	0.06
LV/TL, mg/cm	71.9±2.7	76.2±1.8	0.24
RV/TL, mg/cm	14.0±0.5	14.1±0.7	0.90
Atria/TL, mg/cm	4.8±0.3	5.8±0.4	0.07
Aorta/TL, mg/cm	4.1±0.3	3.4±0.1	0.09
	Female		
n	9	7	
BW, g	20.5±0.3	20.9±0.4	0.43
LV, mg	86.1±3.0	81.4±1.7	0.23
RV, mg	17.9±0.9	15.9±0.5	0.12
Atria, mg	6.6±0.4	5.4±0.8	0.15
LV/TL, mg/cm	50.6±1.6	47.5±0.9	0.15
RV/TL, mg/cm	10.5±0.5	9.3±0.3	0.11
Atria/TL, mg/cm	3.8±0.2	3.1±0.4	0.12
Aorta/TL, mg/cm	3.1±0.2	3.0±0.2	0.97
	All Gender		
n	18	12	
LV/TL, mg/cm	61.3±3.0	61.8±4.1	0.90
RV/TL, mg/cm	12.3±0.5	11.9±0.7	0.70
Atria/TL, mg/cm	4.4±0.2	4.6±0.4	0.67
Aorta/TL, mg/cm	3.6±0.2	3.3±0.1	0.25

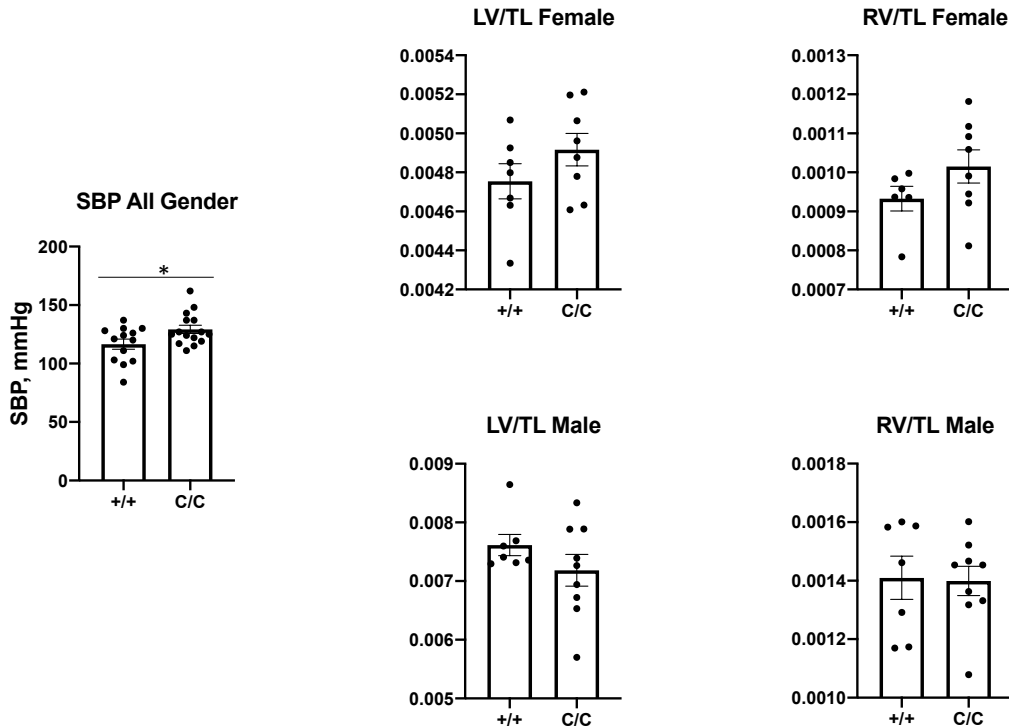


Figure 3.5 Hemodynamic analysis and ventricle weight analysis in MLK3 CRIB (C/C) and wild type (+/+) mice after TAC

3.6 Higher blood pressure in the female MLK3 CRIB mice after TAC

We checked the functional and structural changes after TAC surgery in both MLK3 CRIB mutant and wild type mice by invasive hemodynamics. The data obtained from PV-loops suggests TAC induced significant increased blood pressure in both groups. MLK3 CRIB mice had significantly higher systolic blood pressure (mutant: 129.3 ± 3.6 ; wild type: 116.5 ± 4.298) and diastolic blood pressure (mutant: 72.3 ± 3.8 ; wild type: 58.9 ± 3.0) and also illustrated increased pressure in left ventricle compared to the wild type. However, when analyzed by sex, we observe that the degree of LV pressure overload did not differ between male TAC mice of either genotype, whereas LV systolic pressure in females was higher in MLK3 CRIB mutants compared with female WT TAC mice.

Further, the left ventricle functional markers (LV EDP, Contractile index) were lower in MLK3 CRIB group, indicating the increased cardiac dysfunction in MLK3 CRIB mice. Together, mutation in MLK3 CRIB domain may cause hypertension and lead to increased risk of cardiac functional impairment and remodeling. (Table 3. 5, Figure 3. 5)

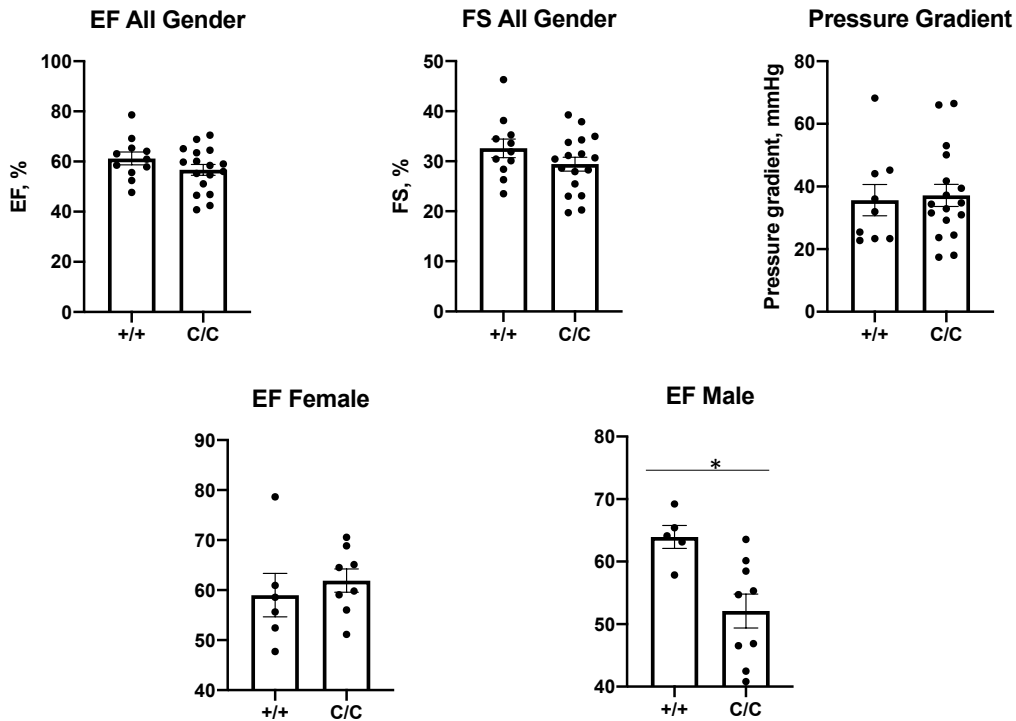


Figure 3.6 Cardiac function analysis in MLK3 CRIB (C/C) and wild type (+/+) mice by echocardiography after TAC

3.7 Decreased cardiac function in MLK3 CRIB mutant mice

Finally, we analyzed the functional and structural changes after TAC surgery in both mutant and wild type mice. Hearts in MLK3 CRIB male mutant mice exhibited decreased ejection fraction and fractional shortening after 7 days of TAC compared to the wild type group, whereas female MLK3 CRIB mice had no differences in these parameters compared with WT. Other cardiac functional

parameters did not differ between genotypes. The pressure gradient was slightly higher in MLK3 CRIB mutant mice compared to the wild type ones, which is also consistent with previous conclusions that MLK3 CRIB domain is important for the regulation of blood pressure. To sum up, after TAC surgery, the hearts of MLK3 CRIB mice had higher blood pressure and also decreased cardiac function. (Table 3.6, Figure 3.6)

3.8 Statement of Contributions

I am grateful to the members in Dr. Robert Blanton Lab, especially Dr. Robert Blanton, Suchita Pande, and Gregory L. Martin. The animal TAC surgery and Pressure- volume loops experiments were done by Gregory L. Martin in MCRI, Tufts Medical Center, Boston, MA. The echocardiography was done by Peiwen Liu (writer). Besides, all the figures and tables are based on the experimental results and all the analysis and the figures were made by Peiwen Liu (writer).

Table 3.5 Hemodynamic analysis in MLK3 CRIB and wild type mice after 25G TAC

	MLK3 CRIB	MLK3 WT	P Value
	Male		
n	8	7	
SBP, mmHg	132.4±5.7	125.4±4.0	0.35
DBP, mmHg	71.88±6.4	61.0±5.1	0.22
MAP, mmHg	119.9±6.5	114.9±4.7	0.54
LV EDP, mmHg	9.4±1.8	14.1±2.0	0.11
LV Dp/dt _{max} , mmHg/s	6752.1±545	5644.0±408	0.13
LV Dp/dt _{min} , mmHg/s	-6297.0±521	-5072±373	0.08
Contractile index, s ⁻¹	192.1±8.1	212.1±6.6	0.08
Stroke Volume, µl	22.0±1.6	19.1±2.6	0.37
Cardiac Output, µl/min	12047±931	10224±1382	0.30
	Female		
n	7	6	
SBP, mmHg	125.7±4.0	84.0±5.8	0.02
DBP, mmHg	72.7±4.2	56.3±2.6	<0.01
MAP, mmHg	113.7±3.8	98.8±5.4	0.05
LV EDP, mmHg	11.8±1.7	8.7±2.3	0.30
LV Dp/dt _{max} , mmHg/s	6601.2±432	5891.5±549	0.33
LV Dp/dt _{min} , mmHg/s	-5845.3±477	-5374.7±812	0.63
Contractile index, s ⁻¹	200.6±8.7	206.3±9.4	0.67
Stroke Volume, µl	24±4.2	21.8±2.3	0.66
Cardiac Output, µl/min	13378±2313	11702±1153	0.53
	All gender		
n	15	13	
SBP, mmHg	129.3±3.6	116.5±4.298	0.03
DBP, mmHg	72.3±3.8	58.9±3.0	0.01
MAP, mmHg	117.0±3.9	107±4.1	0.10
LV EDP, mmHg	10.5±1.3	11.62±1.6	0.61
LV Dp/dt _{max} , mmHg/s	6682.5±341	5758±323	0.06
LV Dp/dt _{min} , mmHg/s	-6089±348	-5212±407	0.12
Contractile index, s ⁻¹	196±5.8	209±5.4	0.11
Stroke Volume, µl	22.9±2.0	20.4±1.7	0.35
Cardiac Output, µl/min	12661±1140	10906±902	0.24

Table 3.6 Cardiac structure and function in MLK3 CRIB and wild type mice after 25G TAC

	MLK3 CRIB	MLK3 WT	P Value
Male			
n	9	5	
Ejection Fraction, %	52.11±2.72	63.95±1.84	0.01
Fractional Shortening, %	26.45±1.69	34.32±1.30	<0.01
IVS; d, mm	1.07±0.04	1.182±0.06	0.12
LVID; d, mm	3.88±0.10	3.88±0.08	0.98
LVID; s, mm	2.86±0.11	2.55±0.10	0.10
LVPW; d, mm	1.06±0.04	0.98±0.02	0.21
AV peak velocity, m/s	3.16±0.18	3.24±0.34	0.78
Pressure gradient, mmHg	40.86±4.58	43.74±9.11	0.75
Female			
n	8	6	
Ejection Fraction, %	61.88±2.33	58.99±4.36	0.54
Fractional Shortening, %	32.79±1.65	31.14±2.27	0.63
IVS; d, mm	1.00±0.03	0.93±0.02	0.16
LVID; d, mm	3.64±0.05	3.68±0.05	0.53
LVID; s, mm	2.44±0.06	2.54±0.14	0.50
LVPW; d, mm	0.91±0.04	0.89±0.07	0.77
AV peak velocity, m/s	2.81±0.22	2.67±0.18	0.67
Pressure gradient, mmHg	32.98±5.39	29.12±4.12	0.62
All Gender			
n	17	11	
Ejection Fraction, %	56.71±2.13	61.25±2.53	0.19
Fractional Shortening, %	29.74±1.40	32.59±1.86	0.18
IVS; d, mm	1.04±0.03	1.05±0.05	0.83
LVID; d, mm	3.77±0.06	3.77±0.05	0.93
LVID; s, mm	2.66±0.08	2.55±0.08	0.36
LVPW; d, mm	0.99±0.03	0.93±0.04	0.27
AV peak velocity, m/s	2.99±0.14	2.93±0.20	0.80
Pressure gradient, mmHg	37.15±3.54	35.61±5.01	0.80

Chapter 4: Discussion

In the current study, we have identified that mutation of the MLK3 CRIB domain leads to: 1) increased blood pressure and basal LV hypertrophy in unstressed mice, and 2) no change in LV hypertrophy after pressure overload by TAC, but reduction of LV systolic function as assayed on echocardiography. We interpret these findings to support a novel role of the MLK3 CRIB domain in the maintenance of cardiovascular homeostasis in vivo.

Several studies indicate that the cGMP-dependent protein kinase I α opposes cardiac dysfunction and remodeling. However, the results of clinical trials using PKG activating drugs in HF patients were inconsistent. To address this discordance, we have explored downstream substrates of PKG which might serve as better therapeutic targets in HF. Our previous investigations also reveal that MLK3 interacts with PKG and acts as a PKGI α kinase substrate. In our previous study, we observed quite significant effects of whole body MLK3 deletion (MLK3^{-/-}) on LV structure and function. Specifically, there was increased cardiac dysfunction after pressure overload in MLK3^{-/-} mice by echocardiography, hemodynamic analysis, and histological assays of cardiomyocyte hypertrophy and fibrosis (3). This supported our hypothesis: MLK3 opposes the LV pathological hypertrophy, dysfunction and remodeling in heart after pressure overload. In the current study, to disrupt MLK3 kinase activation, we studied the MLK3 CRIB mutant mice model, which has point mutation disrupting the MLK3 CRIB domain. We observed abnormal higher blood pressure and cardiac hypertrophy in MLK3 CRIB mice in the baseline state, and also observed decreased LV JNK

activation state, decreased CD31 expression and reduced MLK3 expression. Further, in the setting of LV pressure overload, we observed increased hypertension in female CRIB mutant mice, and pathological dysfunction in heart after pressure overload in the male CRIB mutant mice. Overall the results suggest that the MLK3 CRIB domain is important for MLK3 kinase activation in opposing LV dysfunction and remodeling, but the kinase-independent mechanism of MLK3 still remains unknown. To further determine the mechanisms and requirements of MLK3 kinase activity, the protein expressions, such as JNK, MLK3, RhoA and CD31, should also be analyzed after 7 days after TAC surgery; histological analysis of the LV tissue collected in this study for cardiomyocyte size, fibrosis and capillary density may give us more evidence of the mechanism in physical fact, including fibrosis and angiogenesis.

In fact, as a mediator of JNK activation, the MLK3 is expressed throughout the body, in multiple cell types, indicating the MLK3 kinase may have whole body effect. Others have reported that MLK3 knockout mice are protected against diet-induced steatohepatitis (22). MLK3 is also involved in tumorigenesis (23) and cancer cell migration (24). Besides, MLK3 also has an effect on the immune system (25). These results all indicate MLK3 can be a novel therapeutic target in many fields in the future. It is also interesting to note that while in our study mutation of MLK3 led to a more severe cardiovascular disease phenotype, several other studies above support that MLK3 disruption protects against other disease models. These findings suggest that MLK3 may exert protective versus

pathologic effects in various tissues and in response to different pathologic stimuli.

In previous reports, the small GTPase Cdc42 also shows antihypertrophic effects in mouse heart. Cdc42 was observed to be specifically activated after pressure overload in mouse heart and cultured cardiomyocytes. After pressure overload, the mice with heart-specific deletion of Cdc42 developed worsened cardiac hypertrophy and quickly transitioned to heart failure compared with WT controls (26). These findings indicated the loss of activation of Cdc42- JNK pathways enhanced the pathological cardiac dysfunction and led to heart failure. As we mentioned in the introduction, Cdc42 is also one of the important activators of MLK3. Importantly, the activation of MLK3 kinase requires the interaction of Cdc42 with MLK3's CRIB motif. In our study, we found out that the MLK3 CRIB domain is critical for regulating the LV structure and function. Together, these results support that the Cdc42- mediating MLK3 is a novel antihypertrophic and cardiac functional regulatory signaling pathway.

There are some limitations in this study. Although the mice used in this study were of the same age, the female mice were smaller in size and weighed less than the male, which means they also have smaller organs, such as heart and aorta, and this may impact the severity of TAC surgery. Second, in our TAC study, female MLK3 CRIB mutant mice displayed increased LV pressure compared with WT mice, which is unexpected as the TAC procedure generally raises blood pressure to the same extent between genotypes. On more specific analysis, we observed that blood pressure was elevated in the CRIB mutant female TAC mice, but not in

female WT TAC mice. We hypothesize that the smaller size of the female mice reduced the degree of pressure overload, owing to the reduced constriction of the 25G needle around the smaller aortic diameter. Besides, while using the 25G TAC surgery model, which is a mild choice for pressure overload to restrict the aorta, it is likely that the surgery had limited effect on the females when the aortas and hearts were of smaller size. In this study we only observed and measured the parameters on day 7 after TAC surgery, which represents a relatively early time point. Thus, we cannot determine from this study the specific effects of the MLK3 CRIB domain on longer duration of LV pressure overload, and would need to do additional studies, such as 4 or 8-week TAC. Finally, additional data will be helpful to support further the conclusions of this study that the MLK3 CRIB domain opposes pathological LV hypertrophy and remodeling. Specifically, analysis of pathologic gene expression and protein level in hearts, and also histological assays for cardiomyocytes hypertrophy and fibrosis, will provide more details on how MLK3 kinase-dependent and independent mechanisms regulate LV hypertrophy and remodeling.

In conclusion, the findings from this study identify that mutation of the MLK3 CRIB domain leads to hypertension, LV hypertrophy, and LV dysfunction to pressure overload. This study also demonstrates that the MLK3 CRIB mutation leads to reduced LV JNK signaling. We conclude that the MLK3 CRIB domain is of critical importance in the regulation of LV structure and function. These findings therefore suggest that modulation of MLK3 CRIB domain may represent a therapeutic strategy for conditions such as LV hypertrophy and remodeling.

Chapter 5: Bibliography

1. Levy D, Garrison RJ, Savage DD, Kannel WB, Castelli WP. Prognostic implications of echocardiographically determined left ventricular mass in the Framingham Heart Study. *N Engl J Med* 322: 1561–1566, 1990. doi:10.1056/NEJM199005313222203.
2. Lakka H, Laaksonen DE, Lakka TA, et al. The Metabolic Syndrome and Total and Cardiovascular Disease Mortality in Middle-aged Men. *JAMA*. 2002;288(21):2709–2716. doi:10.1001/jama.288.21.2709
3. Calamaras TD, Baumgartner RA, Aronovitz MJ, et al. Mixed lineage kinase-3 prevents cardiac dysfunction and structural remodeling with pressure overload. *Am J Physiol Heart Circ Physiol*. 2019;316(1):H145–H159. doi:10.1152/ajpheart.00029.2018
4. James T. Willerson, The Medical and Device-Related Treatment of Heart Failure. *Circ Res*. 2019 May 24; 124(11): 1519. doi: 10.1161/CIRCRESAHA.119.315268
5. Kong Q, Blanton RM. Protein kinase G I and heart failure: Shifting focus from vascular unloading to direct myocardial antiremodeling effects. *Circ Heart Fail*. 2013;6(6):1268–1283. doi:10.1161/CIRCHEARTFAILURE.113.000575
6. Xue M., Li T., Wang Y., Chang Y., Cheng Y., Lu Y., et al. (2019). Empagliflozin prevents cardiomyopathy via sGC-cGMP-PKG pathway in type 2 diabetes mice. *Clin. Sci. (Lond)* 133, 1705–1720. 10.1042/CS20190585. doi.org/10.1042/CS20190585
7. Hofmann F. The biology of cyclic GMP-dependent protein kinases. *J Biol Chem*. 2005;280:1–4. DOI: 10.1074/jbc.R400035200
8. Craige SM, Chen K, Blanton RM, Keaney JF Jr, Kant S. JNK and cardiometabolic dysfunction. *Biosci Rep*. 2019;39(7):BSR20190267. Published 2019 Jul 18. doi:10.1042/BSR20190267
9. Bassi R, Heads R, Marber MS, Clark JE. Targeting p38-MAPK in the ischaemic heart: kill or cure? *Curr Opin Pharmacol*. 2008 Apr;8(2):141–6. doi.org/10.1016/j.coph.2008.01.002
10. Kant S, Barrett T, Vertii A, et al. Role of the mixed-lineage protein kinase pathway in the metabolic stress response to obesity. *Cell Rep*. 2013;4(4):681–688. doi:10.1016/j.celrep.2013.07.019
11. Kant S, Standen CL, Morel C, et al. A Protein Scaffold Coordinates SRC-Mediated JNK Activation in Response to Metabolic Stress. *Cell Rep*. 2017;20(12):2775–2783. doi:10.1016/j.celrep.2017.08.025
12. Liang Q, Bueno OF, Wilkins BJ, Kuan CY, Xia Y, Molkenin JD. c-Jun N-terminal kinases (JNK) antagonize cardiac growth through cross-talk with calcineurin-NFAT signaling. *EMBO J*. 2003;22(19):5079–5089. doi:10.1093/emboj/cdg474
13. Lal H, Verma SK, Golden HB, Foster DM, Smith M, Dostal DE. Stretch-induced regulation of angiotensinogen gene expression in cardiac myocytes and fibroblasts: opposing roles of JNK1/2 and p38alpha MAP

- kinases. *J Mol Cell Cardiol.* 2008;45(6):770–778.
doi:10.1016/j.yjmcc.2008.09.121
14. Gallo K. A., Mark M. R., Scadden D. T., Wang Z., Gu Q., Godowski P. J. Identification and characterization of SPRK, a novel src-homology 3 domain-containing proline-rich kinase with serine/threonine kinase activity. 1994; *J. Biol. Chem.* 269:15092–15100
 15. Hehner SP, Hofmann TG, Ushmorov A, et al. Mixed-lineage kinase 3 delivers CD3/CD28-derived signals into the I κ B kinase complex. *Mol Cell Biol.* 2000;20(7):2556–2568. doi:10.1128/mcb.20.7.2556-2568.2000
 16. Burbelo P. D., Drechsel D., Hall A. A Conserved Binding Motif Defines Numerous Candidate Target Proteins for Both Cdc42 and Rac GTPases. 1995; *J. Biol. Chem.* 270:29071–29074.
 17. Teramoto H., Coso O. A., Miyata H., Igishi T., Miki T., Gutkind J. S. Signaling from the small GTP-binding proteins Rac1 and Cdc42 to the c-Jun N-terminal kinase/stress-activated protein kinase pathway. A role for mixed lineage kinase 3/protein-tyrosine kinase 1, a novel member of the mixed lineage kinase family. 1996; *J. Biol. Chem.* 271:27225–27728.
 18. Bock B. C., Vacratsis P. O., Qamirani E., Gallo K. A. Cdc42-induced activation of the mixed-lineage kinase SPRK in vivo. Requirement of the Cdc42/Rac interactive binding motif and changes in phosphorylation. 2000; *J. Biol. Chem.* 275:14231–14241.
 19. Gallo, K., Johnson, G. Mixed-lineage kinase control of JNK and p38 MAPK pathways. *Nat Rev Mol Cell Biol* 3, 663–672 (2002).
doi.org/10.1038/nrm906
 20. Kant S, Swat W, Zhang S, et al. TNF-stimulated MAP kinase activation mediated by a Rho family GTPase signaling pathway. *Genes Dev.* 2011;25(19):2069–2078. doi:10.1101/gad.17224711
 21. Richards DA, Aronovitz MJ, Calamaras TD, et al. Distinct Phenotypes Induced by Three Degrees of Transverse Aortic Constriction in Mice. *Sci Rep.* 2019;9(1):5844. Published 2019 Apr 10. doi:10.1038/s41598-019-42209-7
 22. Ibrahim SH, Gores GJ, Hirsova P, et al. Mixed lineage kinase 3 deficient mice are protected against the high fat high carbohydrate diet-induced steatohepatitis. *Liver Int.* 2014;34(3):427–437. doi:10.1111/liv.12353
 23. Chadee DN. Involvement of mixed lineage kinase 3 in cancer. *Can J Physiol Pharmacol.* 2013 Apr;91(4):268-74. doi: 10.1139/cjpp-2012-0258. Epub 2012 Dec 19.
 24. Fei Zhang, Yu Zhu, Dong Yang, et al. MLK3 is a newly identified microRNA-520b target that regulates liver cancer cell migration. *PLoS One.* 2020 Mar 26;15(3):e0230716. doi: 10.1371/journal.pone.0230716. eCollection 2020.
 25. Kumar S, Singh SK, Rana A, et al. Mixed lineage kinase 3 inhibition induces T cell activation and cytotoxicity. *Proc Natl Acad Sci U S A.* 2020 Mar 24. pii: 201921325. doi: 10.1073/pnas.1921325117.

26. Maillet M, Lynch JM, Sanna B, York AJ, Zheng Y, Molkentin JD. Cdc42 is an antihypertrophic molecular switch in the mouse heart. *J Clin Invest.* 2009;119(10):3079–3088. doi:10.1172/JCI37694